Development of a 'Fish Tail' Rudder to Improve a Ship's Maneuverability in Seaway

Aries Sulisetyono

Abstract*—The maneuverability of a ship at seaway is strongly influenced by a design of rudder. An innovative design of rudder based on a tail shape of fish was developed with the intent of improving an efficiency of ship maneuverability. Two designs of rudders were proposed i.e. the rudder of forked which is a rudder with an area reduction on the middle part, and the lanceolate shape or a rudder with additional area on the middle part. In evaluation of the rudder designs performance, the numerical approach of Computational Fluid Dynamic (CFD) was applied to determine a side force generated by rudder using the commercial software of FLUENT. Numerical simulations were performed on the rudder designed of rectangular, forked and lanceolate which had similar a surface area with the variations of rudder angle such as 100, 200 and 300 due to the uniform fluid flow at a constant speed. Further simulations was performed on the two forked rudder designed which takes into account the influence of propeller due to fluid flow on the rudder surface. It had shown the velocity of fluid flow behind the shaft of propeller very small in which the middle part of the rudder produced less lift force compare to the other part of rudder. Mathematical and numerical model of ship maneuvering were developed in order to evaluate the performance of a ship maneuvering in seaway based on the IMO standards on turning test. The simulation results had shown the rudder of forked produce the ship maneuvering performance that exceeds the performance of rectangular rudder as well as lanceolate rudder.

Keywords—rudder, computational fluid dynamics, ship maneuverability.

I. Introduction

Maneuverability of ship is an important aspect considers avoiding collision accident of ships in seaway especially in the restricted area of waterway. The International Maritime Organization (IMO) has published the safety regulation in terms of manoeuvrability criteria that must be owned by every ship [1].

The ability of a ship while doing manoeuvre at seaway is strongly depends to device of rudder in generating lift or side force. Actually, the work principle of rudder had similarity with a function of fish tail in navigation fish's body in seaway. There are several types of fish tail such as the shape of Forked, Lunate, Truncated rounded, Lanceolate and Eel-like. In this paper, an innovative design of rudders based on the two types of fish's tail such as Forked and Lanceolate were proposed to enhance manoeuvring performance of ship. Forked rudder is defined a rudder with a reduction area on the middle part of rudder's tail, and Lanceolate rudder is a rudder with an additional area on the middle part of rudder's tail, The lift coefficient of rudder design should be firstly defined by using computational fluid dynamic (CFD) following [2]. The principle of uniform flow on behind of propeller was considered to figure out a flow pattern around a rudder. In addition the principle of fluid flow in front of the propeller that the velocity of water flow in the upper area of the blade propeller have the greatest value and gradually decreases to near zero at the propeller shaft [3], as shown in Figure 1. Therefore the area of the rudder in front of the propeller which is in line with the shaft propeller would have a small value of flow velocity compare to upper and lower are of rudder.

Aries Sulisetyono is with Department of Naval Architecture and Shipbuilding Engineering, Faculty of marine Technology, Institut Teknologi Sepuluh Nopember, Surabaya, 60111, Indonesia. Email: sulisea@na.its.ac.id.

In general a ship with a rudder flap had performed manoeuvrability better compare to a ship with a conventional rudder in the same wetted area of rudder [4]. The additional flap on rudder to be considered evaluated in this paper to investigate the effect of flap in increasing lift or side force to a conventional rudder.

Furthermore, the manoeuvring program was developed based on clarke's equation [5] with some modification to into account a lift coefficient of rudder which as independent input. The numerical test was conducted against three designs of rudders i.e. rectangular, forked and lanceolate, and alls were also designed with and without flap which had a same value of wetted surface area.

II. Method

A. Calculation of Lift Coefficient

The cross-flow problems of the 3D rudder were solved by using CFD software. In the numerical simulation, the flow was assumed to be uniform, steady, and incompressible. The fluid density (ρ) of the water as the working fluid was 1025 kg/m^3 and viscosity (μ) = 1.003 10^{-3} kg/m sec. The rudder size was modeled in the CFD geometry with the certain value of chord (c) and span (l), and the foil section of seri NACA 0018.

The 6-variations of the rudder design were introduced such as Model 1: rectangle with flap, Model 2: forked with flap, Model 3: lanceolate with flap, Model 4: rectangle without flap, Model 5: forked without flap, and Model 6: lanceolate without flap, as shown in Figure 2. For the sake of performance comparison, all models were designed in the same value of surface area (A) about 25.2 m^2. The flap areas of models were determined about 30% of surface areas of models as recommended by [6].

Fluid boundary condition that was used in modeling as has been illustrated in Figure 3 while the length 5 x c m, height 3 x l m, and width 5 x c m. The 3D rudder models had been simulated in three variations of rudder angle (δ) such as 100, 200 and 350 due to incoming uniform flow with the velocity (u) of 6 m/s. The

boundary conditions of rudder model were determined while pressure hold on the boundaries of rudder geometry. Grid independence tests was carried out to obtain the most efficient number of elements in producing good accuracy of output with time consuming a short as possible. Numerical tests were conducted with variety number of elements i.e. 678027, 701659, 730564 and 762337. The grid independence test was performed on the model A, in which the computational result shown a steady condition occured since the element number of 730564. While the procedure of computational was conducted properly, the lift coefficient (Cl) of rudder could be obtained by equation (1).

$$Cl = \frac{Lift}{\frac{1}{2}\rho A u^2} \tag{1}$$

The lift or force of rudder was determined with finding the difference of pressure distribution between the top and bottom side of along the rudder's surface. These CFD simulations were conducted on the PC computer with specification: Duo Core Processors 2.0 GHz, Three (3) GB of RAM, and 256 MB graphics card.

B. Calculation of Ship Maneuvering

The evaluation of 6-model rudders performance affect to the ship maneuvring performance was determined following [7]. In this computation, the 6-models of rudders was installed on the ship which have the main dimension of length between perpendicular (*L*) 99 m, width moulded (*B*) 18.785 m, draft (*T*) 6.052 m, and block coefficient (C_b) 0.773. Steady turning test was performed to evaluate ship maneuvering performance. Figure 3 describes the model of turning test, in which the ship was initiated turning with a rotating of rudder for certain degree of angle i.e. 10^0, 20^0 and 35^0. Moreover, the performance of ship maneuvering could be identified with measuring a distance of Advance (*Ad*), Transfer (*Tr*), Tactical Diameter (*TD*), Steady Turning Diameter (*STD*) in the turn for any rudder angle (see Figure 4). In the stage of turning test is divided into four main stages, the first stage of the preparation, which at this stage the ship moves straight from rest until it reaches the desired speed. At this stage there is no turn by rudder, and this phase ends when the rudder has started rotate. The second stage begins when the ship's rudder rotated to form the desired angle and the ending of stage while a ship's direction was about 90^0 to the early direction. The third stage begins when the rudder angle has reached the maximum angle, and the ending of state in sign of the direction of ship about 180^0 or opposite direction to the early stage. And the last stage there is a balance that makes the ship turn around with fixed radius or often referred to as the phase of steady turning.

International Maritime Organization (IMO) set rules regarding the standardization of ship maneuver-ability and it can be referenced in the process of ship design. Based on these standards are required to have the ship. The ship maneuverability criteria set out in the IMO regulations are ability turning, course keeping, yaw checking, and stopping. In the case of turning test, the distance of Advance (Ad) must not more than 4.5 times the length of ship and the tactical diameter (TD) must not more than 5 times the length of ship.

The simulation program was developed based [5] in which the lift coefficient was required as input. The hydrodynamic coefficients of maneuvering were defined by equation (2).

$$\begin{aligned}
Y_{\dot{v}}' &= -\pi\left(\frac{T}{L}\right)^2\left[1+0.16C_b\frac{B}{T}-5.1\left(\frac{B}{L}\right)^2\right]\\
Y_{v}' &= -\pi\left(\frac{T}{L}\right)^2\left[1+0.4C_b\frac{B}{T}\right]\\
Y_{\dot{r}}' &= -\pi\left(\frac{T}{L}\right)^2\left[0.67\frac{B}{L}-0.0033\left(\frac{B}{T}\right)^2\right]\\
Y_{r}' &= -\pi\left(\frac{T}{L}\right)^2\left[-0.5+2.2\frac{B}{L}-0.08\frac{B}{T}\right]\\
N_{\dot{v}}' &= -\pi\left(\frac{T}{L}\right)^2\left[1.1\frac{B}{L}-0.041\frac{B}{T}\right]\\
N_{v}' &= -\pi\left(\frac{T}{L}\right)^2\left[0.5-2.4\frac{T}{L}\right]\\
N_{\dot{r}}' &= -\pi\left(\frac{T}{L}\right)^2\left[\frac{1}{12}+0.017C_b\frac{B}{T}-0.33\frac{B}{L}\right]\\
N_{r}' &= -\pi\left(\frac{T}{L}\right)^2\left[0.25+0.039\frac{B}{T}-0.56\frac{B}{L}\right]
\end{aligned} \tag{2}$$

Where $Y_{\dot{v}}', Y_{\dot{r}}', Y_v', Y_r', N_{\dot{v}}', N_{\dot{r}}', N_v',$ and N_r' are non – dimensional hydrodynamic coefficients. Hydrodynamic coefficient which has related to the rudder force is the value of Y_{δ}', influence to the ship's maneuvering performance, and it can be calculated by equation (3).

$$Y_{\delta}^{'} = \left(\frac{S}{LT}\right)\left(\frac{T}{L}\right)\left(\frac{dCl}{d\delta}\right)Cl\left(\frac{u_a}{u}\right)^2 \tag{3}$$

Where S is surface area of rudder, *Cl* is lift coefficient, and u_a is a flow velocity on rudder surface. Since the rudder position is assumed a half of ship length after of amidships, non-dimensional rudder moment of N_{δ}' can be calculated by equation (4).

$$N_{\delta}^{'} = 0.5Y_{\delta}^{'} \tag{4}$$

The steady turning diameter (*STD*) of the ship while perform a turning movement can be approximated by using equation (5) as follow as.

$$STD = \frac{L}{\delta}\frac{\left(Y_v^{'}N_r^{'} - N_v^{'}\left(Y_r^{'} - m^{'}\right)\right)}{N_v^{'}Y_{\delta}^{'} - Y_v^{'}N_{\delta}^{'}} \tag{5}$$

Where *m* is mass of ship and δ is rudder angle. The indicator of maneuvering performance based on IMO regulation such as tactical diameter (*TD*), advanced (*Ad*) and transfer (*Tr*) were approximated by equation (6) refer to [5].

$$\begin{aligned}
\frac{TD}{L} &= 0.140 + 1.0\frac{STD}{L}\\
\frac{Ad}{L} &= 1.10 + 0.514\frac{TD}{L}\\
\frac{Tr}{L} &= 0.375 + 0.531\frac{TD}{L}
\end{aligned} \tag{6}$$

III. Result and Discussion

The results of the CFD simulation on six (6) models type of rudder using either flap or without flap for a

rudder angle of 100, 200, and 300 were presented in Figures 5 – 10 respectively. Figures 5 - 10 shown the distributions of pressure on all type of models while the rudder was rotated about 100 , 200, and 350 respectively due to uniform flow with the velocity about 6 m/s. It is shown the models with flap had pressure higher than models without flap. In general, the model of rudder with flap had also higher lift coefficient compare to the rudder without flap for all conditions of rudder angle. Because of the additional flap on rudder gave contribution significantly to increase a velocity of fluid flow on top side of rudder's tail and made decreasing of flow velocity on bottom side of rudder's tail. Figures 5 - 10 explained that high pressure distribution concentrate on the leading part of rudder for rudder angle of 100. The high pressure distribution was concentrated on the flap or tail of rudder for case of rudder angle 200 as shown in Figure 7 and 8. The high pressure distribution was spread to the surface of rudder while the rudder angle of 350, even the leading area had higher pressure than the area of tail. The maximum value of lift coefficient for all type of rudder due to the rudder angle of 100, 200 and 350 were described respectively in Table 1.

Figures 11 and 12 described the distribution pressure on the bottom side of models while the rudder angle was rotated about 200. It shown there were the differences of pressure distribution between top side as presented in Figures 7 and 8, and the bottom side of rudder. The top side of rudder had a higher pressure than the bottom side because the velocity of fluid flows on top side faster than the bottom side.

As presented in Table 1, the lift coefficient for all of models was increased while the rudder angle was rising up to 350 which is the maximum degree of rudder angle according IMO regulation. It also shown in Table 1 that the type rudder of Forked (Model 2 and Model 5) gave a lift coefficient higher than others on both conditions of with and without flap for all rudder angles. Except Model 5 while the rudder angle was 100, generated lift force lower compare to Model 4. It shown the rudder's tail of Model 5 was not affect yet to increase a velocity of fluid flow on the top of rudder's tail area. Since the length of Model 5 was longer compare to Model 4, the rudder's tail of Model 5 had contributed to increase lift force while the rudder angle was above 100.

Furthermore, while the effect of propeller was into accounted in the CFD simulation, it means fluid flow was not uniformly around the rudder, the pressure distribution of rudder had been significant changed. The middle part of the rudder area which was a line position to the shaft of propeller had a small value of lift, because the velocity of flow stream on middle part was small value compare to the other part of rudder. This is consistent with the explanation of the study conducted by [3], that the velocity of fluid flow after or behind the upper and lower regions of propeller had high value and small value on the area of the propeller shaft. The pressure distribution on the rudder due to fluid flow which was the propeller effect considered as presented in Figure 13. In this simulation, the middle part of rudder which was located in front of the shaft propeller, was installed a tube, and uniform flow with the same velocity, 6 m/s was streamed against to the model. The result of CFD simulation was described in Figure 13.

The contour of fluid flow on the x-axis as shown in Figure 8 illustrated the middle part of rudder's tail had the smallest value of fluid pressure. This phenomenon explained that the middle part of a tail rudder did not give a lift force maximally so it might be removed, and the type rudder of Forked with flap (Model 2) was the most optimal type of the rudder. In other hand, the reduction on the middle part of a tail rudder might influence to the reduction of power to rotate a rudder as well as the cost of manufacture.

By using equations (2) until (6) and the lift coefficient obtained by CFD method as shown in Table 2, it can be estimated the value of turning diameter, tactical diameter, advance, and transfer as described in Table 2. In this case, the model with flap was arranged with additional flap angle of 100. It had shown on Table 2 the effect of rudder angle, as well as the effect of rudder shape to the ship maneuvering performance in turning test. In order to see differences in the performance of each rudder type clearly, then the value of turning diameter, tactical diameter, advance, and transfers due to maneuvering test were plotted against to the rudder angle of 100, 200, and 350, as described respectively in Figure 14 – 17 respectively.

Additional flap on rudder had increased the performance of maneuvering for all conditions of the rudder angle, as shown in Figures 14 - 17. The value of STD, TD, Advance, and transfer had increase for the models with additional flap such as the average value of 38%, 37%, 23%, and 45% for the rudder angle 100 respectively; 24%, 22%, 11%, and 35% for the 200 of rudder angle respectively; and 16%, 14%, 5% and 33% for the rudder angle 350 respectively. Figure 14 - 17 also explained the increasing of rudder angle would raise maneuvering performances for all models.

For rudder angle of 100, the model without flap (Model 5 and Model 6) had a turning diameter about 3.2% and 8.6% higher than a conventional rudder (Model 4) respectively. While the rudder angle was switched to 350, the turning diameter of Model 5 was 3% lower than Model 4, but Model 6 had 0.8% of turning diameter higher than Model 4. It shown Model 5 had better performance compare to Model 6 for all rudder angles condition, and better than Model 4 for rudder angle 200 as well as 350. This phenomenon almost the same as models with flap, the turning diameter of Model 1, 2 and 3 were lower value than Model 4 about 35%, 37% and 29.3% for case 100 of rudder angle and 100 of flap angle. While the rudder angle was increased to 350 for the same value of flap angle 100, the turning diameter of Model 1, Model 2 and Model 3 were about 14%, 16% and 12% lower than Model 4 respectively. This phenomenon shown Model 2 had a better performance in ship maneuvering compare to Model 3 about 8% and 2% for the case of rudder angle 100 and 350 respectively.

III. CONCLUSION

The six (6) rudder design has been proposed in an effort to improve the ship's maneuverability in the seaway. The CFD simulation results against all models explained the forked type of rudder (Model 2 and Model 5) generated the highest value of lift coefficient which was compared to other models. The adding flap about 30% of rudder area for all types of rudders contributed

increasing lift coefficient for all conditions of rudder angle. While the existence of the propeller located in front of rudders was considered in the CFD simulation, it was seen the distribution of the pressure at the middle part of the rudder had smaller value than the top or bottom part of the rudder. This phenomenon explained that the model Forked which reduces the middle area, and adding area on the bottom and top of the rudder, had relevance in generating optimally a lift of rudder. Ship maneuvering simulations program was developed to evaluate the maneuverability of ship due to the performance of rudder in which a lift coefficient as input, and output program in terms of turning diameter, tactical diameter, advance and transfer. In over all simulation shown the model 2 had the best performance in ship maneuverability compared to others.

AKNOWLEDGEMENT

The author would like to express thanks to Hardina Mulyasari for helping do simulations using CFD.

REFERENCES

[1] J.M.J Journee and J. Pinkster, "Introduction in Ship Hydromechanics", *Lecture Note*, Delft University of Technology, 2002.
[2] A. Sulisetyono and A.F. Nasirudin, "Wind Sail Analysis Using Computational Fluid Dynamics Simulation", *The International Conference on Marine Technology (MARTEC)*, BUET, Dhaka, Bangladesh, 2010.
[3] S.A. Harvald,."Resistance and Propulsion of Ship". Jonh Wiley and Sons, New York, 1978.
[4] V.L. Edward, (Ed). "Motion In Waves and Controllability", *Priciples of Naval Architecture (Vol III)*. Jersey City, 1989.
[5] D. Clarke, P. Gedling, and G. Hine, "The Application of Manoeuvring Criteria in Hull Design Using Linear Theory" Proceedings of RINA, *Spring Meetings*. London, 1982.
[6] A. Sulisetyono, and H. Hermansyah, "Modifikasi daun kemudi tunggal (konvensional) menjadi daun kemudi dengan flap untuk meningkatkan maneuverability kapal", *Seminar Nasional Teori dan Aplikasi Teknologi Kelautan VII, FT Kelautan, IT*, 2007.
[7] C.A. Lyster, and H.L. Knights, "Prediction Equations for Ships' Turning Circles", Trans. NECIES, 1979.

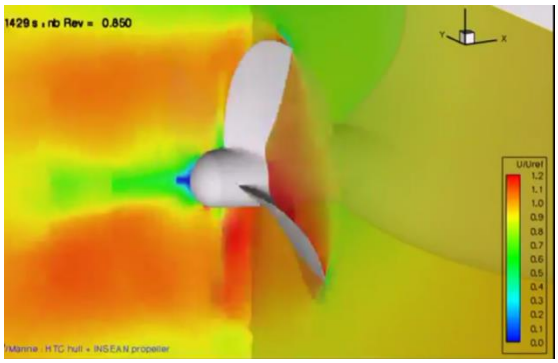

Figure 1. Pressure distribution of flow in front of propeller

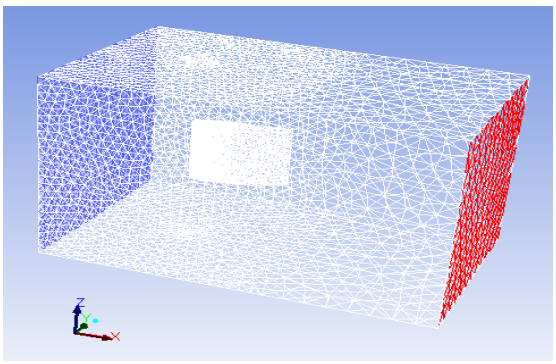

Figure 3. Boundary condition

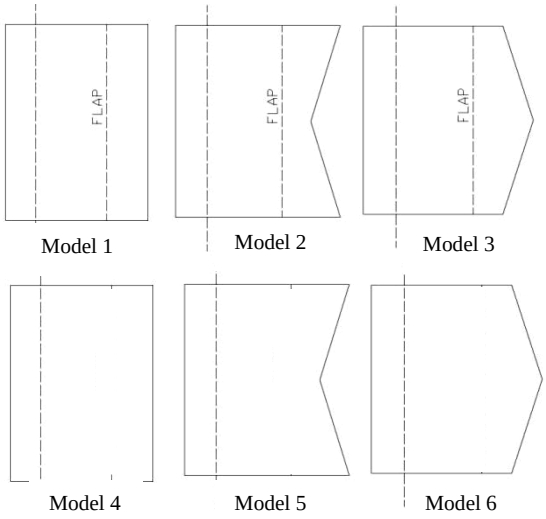

Figure 2. Design of 6-rudders with and without flap

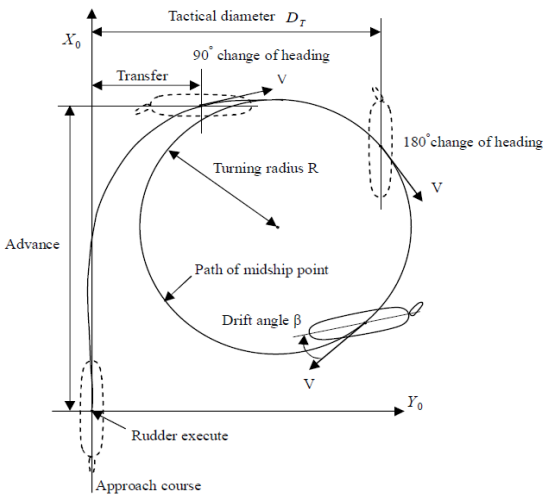

Figure 4. Modeling of turning test

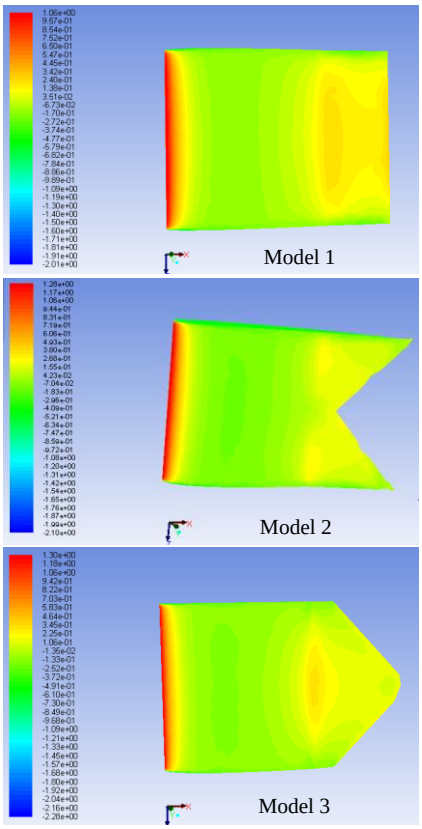

Figure 5. Pressure distribution on top side of model with flap, for rudder angle, 10^0

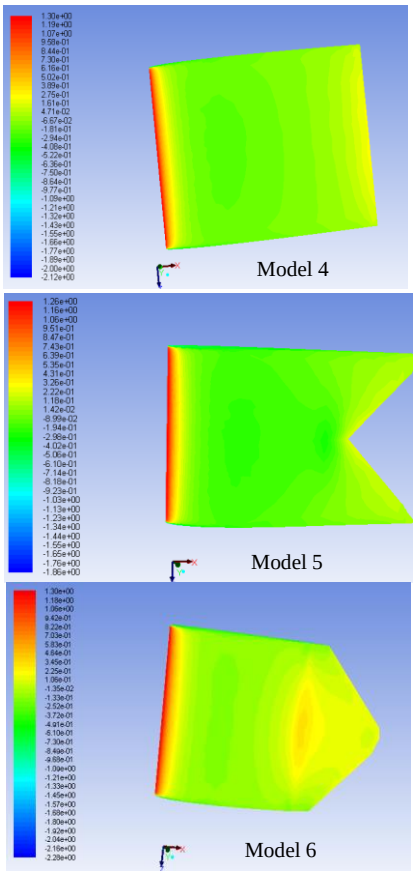

Figure 6. Pressure distributions on top side of model without flap, for rudder angle, 10^0

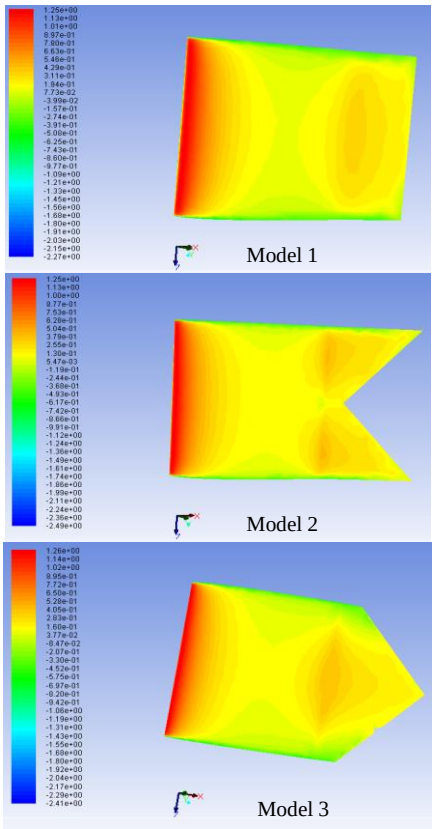

Figure 7. Pressure distributions on top side of model with flap, for rudder angle, 20^0

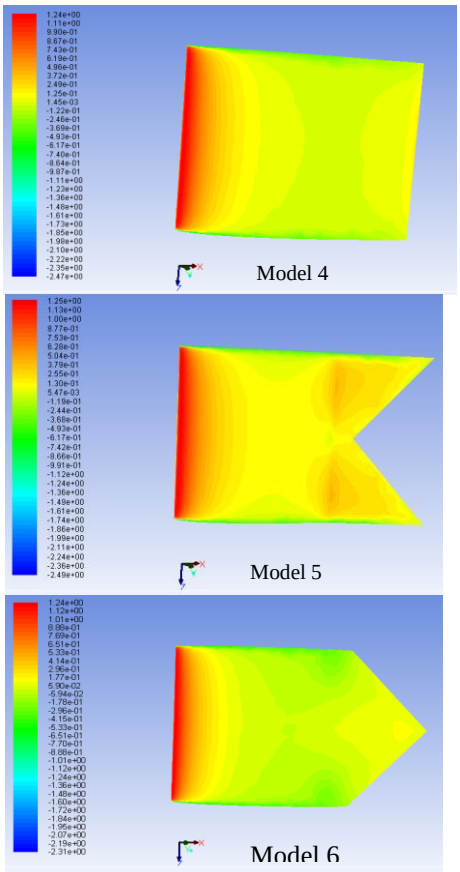

Figure 8. Pressure distributions on top side of model without flap, for rudder angle, 20^0

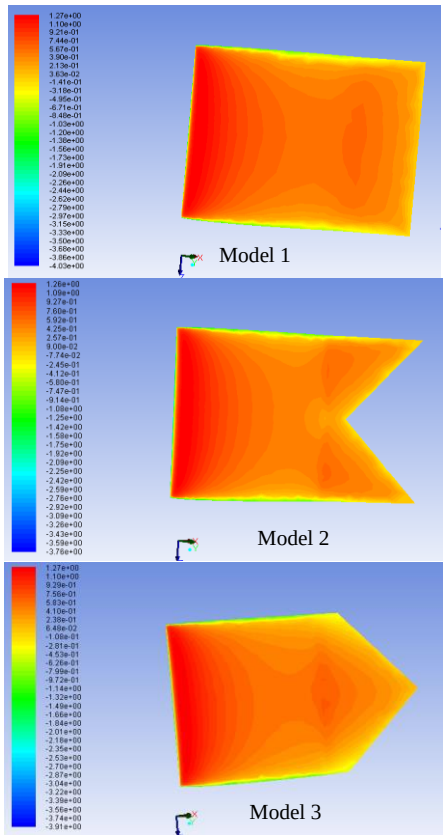

Figure 9. Pressure distributions on top side of model with flap, for rudder angle, 35^0

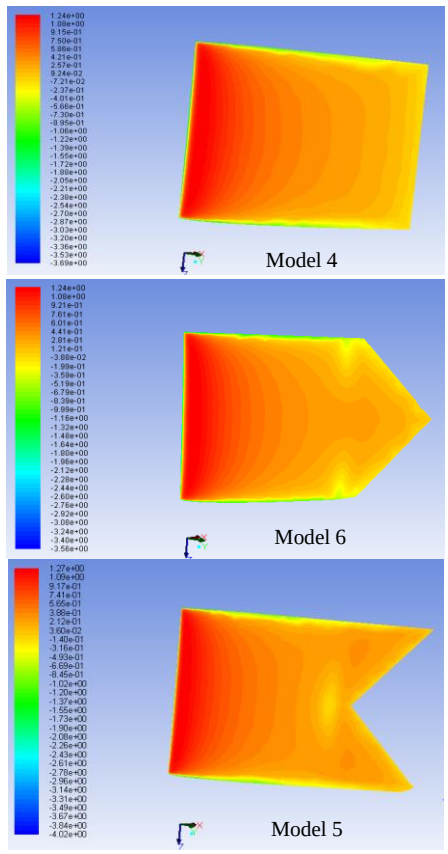

Figure 10. Pressure distributions on top side of model without flap, for rudder angle, 35^0

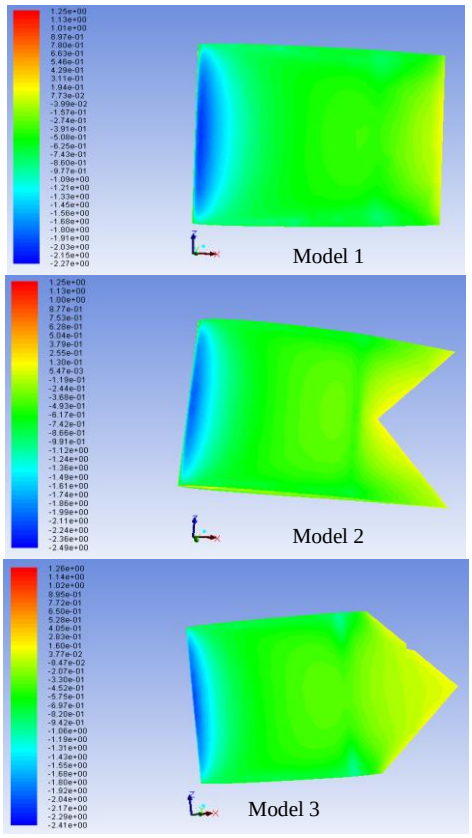

Figure 11. Pressure distributions on bottom side of models without flap, for rudder angle, 20^0

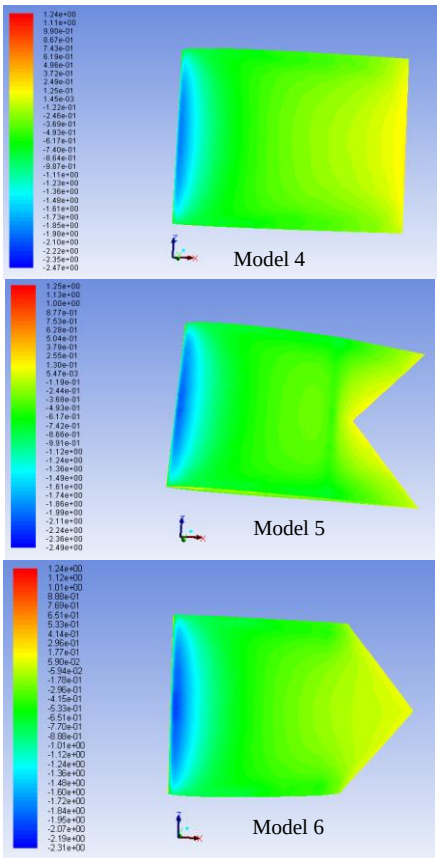

Figure 12. Pressure distributions on bottom side of models without flap,for rudder angle, 20^0

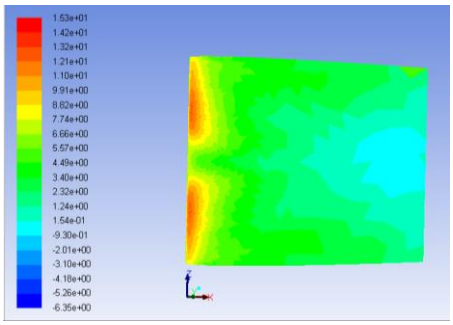

Figure 13. Pressure distributions of rudder with propeller considered

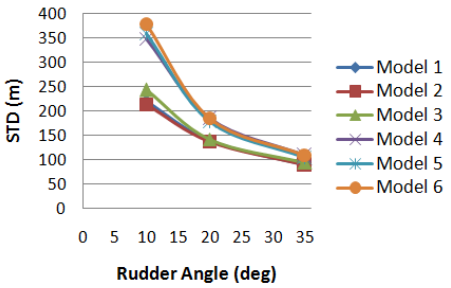

Figure 14. The Steady Turning Diameters due to the angle of rudder

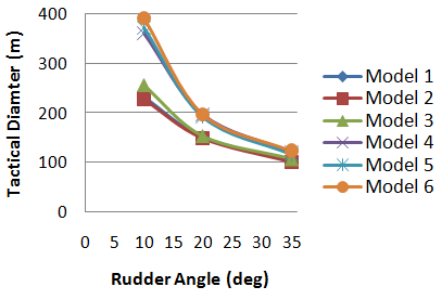

Figure 15. The Tactical Diameters due to the angle of rudder

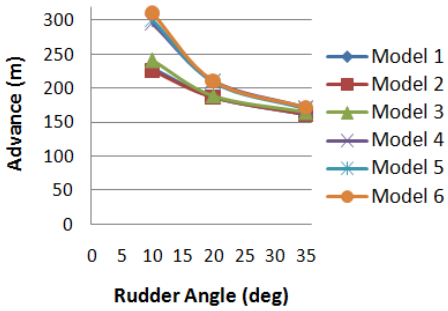

Figure 16. The Advanced distance due to the angle of rudder

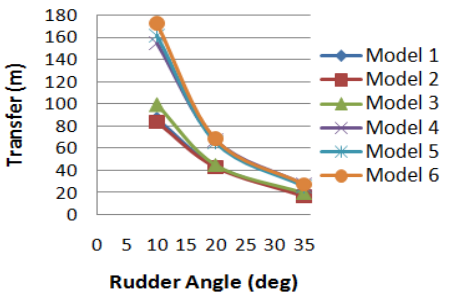

Figure 17. Transfer due to the angle of rudder types

TABLE 1.
LIFT COEFFICIENTS OF RUDDERS

Rudder type	Rudder Angle (δ)°	Lift (KN)	*Cl*
Model 1	10	229.124	0.497
	20	362.557	0.786
	35	564.281	1.223
Model 2	10	235.371	0.510
	20	367.761	0.797
	35	574.135	1.245
Model 3	10	207.294	0.449
	20	357.784	0.776
	35	539.892	1.170
Model 4	10	144.229	0.313
	20	273.529	0.593
	35	468.691	1.016
Model 5	10	139.554	0.303
	20	280.649	0.608
	35	484.822	1.051
Model 6	10	132.335	0.287
	20	273.232	0.592
	35	464.310	1.007

TABLE 2.
MANEUVERING TEST OF 6- RUDDER MODEL

Model	Rudder angle (α)°	STD (m)	TD (m)	Advance (m)	Transfer (m)
1	10	218.929	232.793	228.583	86.479
	20	138.356	152.220	187.168	43.694
	35	88.895	102.759	161.746	17.431
2	10	213.119	226.982	225.596	83.393
	20	136.398	150.262	186.162	42.655
	35	87.370	101.233	160.961	16.620
3	10	241.985	255.849	240.434	98.721
	20	140.202	154.065	188.117	44.674
	35	92.911	106.775	163.810	19.563
4	10	347.795	361.658	294.820	154.906
	20	183.388	197.252	210.315	67.606
	35	107.026	120.889	171.065	27.058
5	10	359.445	373.309	300.808	161.093
	20	178.736	192.599	207.923	65.136
	35	103.465	117.328	169.234	25.167
6	10	379.054	392.917	310.887	171.505
	20	183.588	197.451	210.418	67.712
	35	108.036	121.899	171.584	27.594